

Monolithic Vertical Integration of Si/SiGe HBT and Si-Based Resonant Interband Tunneling Diode Demonstrating Latching Operation and Adjustable Peak-To-Valley Current Ratios

Sung-Yong Chung,^a Niu Jin,^a Ronghua Yu,^b Paul R. Berger,^{a,b}
Phillip E. Thompson,^c Roger Lake,^d Sean L. Rommel^e and Santosh K. Kurinec^f

^aOhio State University, Department of Electrical Engineering, Columbus, OH 43210 USA; ^bOhio State University, Department of Physics, Columbus, OH 43210 USA; ^cNaval Research Laboratory, Code 6812, Washington, DC 20375 USA; ^dDept. of Electrical Engineering, University of California, Riverside, CA 92521 USA; ^eMicroelectronic Engineering Department, Rochester Institute of Technology, Rochester, NY 14623 USA
Phone: (614) 247-6235, FAX: (614) 292-7596, Email: pberger@icee.org

ABSTRACT

We report the first monolithic vertical integration of a Si / SiGe HBT with a Si-based resonant interband tunnel diode (RITD) on a silicon substrate. This enables a 3-terminal negative differential resistance (NDR) device and the resulting devices have the distinguishing characteristics of adjustable peak-to-valley current ratio and adjustable peak current density (PCD) in the collector current under common emitter configuration at room temperature. We experimentally demonstrate its latching property and switching operation based on quantum mechanics.

INTRODUCTION

Integrated circuits combining NDR devices with transistors are of great interest because they have tremendous potential for ultra high speed, and low power consumption. This integration also offers the possibility of greater circuit density. For example, the vertical monolithic integration of an RITD atop the HBT, results in increased functionality per device. NDR devices can be effectively implemented for not only digital logic [1] and memory applications [2], but also high-speed mixed signal applications such as analog-to-digital converters (ADCs) [3] and voltage controlled oscillators (VCOs) [4] for generating sine wave signals.

Peak-to-valley current ratios (PVCR), peak current densities (PCD) and voltage ranges corresponding to the NDR region are the figures-of-merit characterizing NDR devices. To date, tunnel diodes with peak-to-valley current ratios of 6 [5] and peak current densities of 151 kA/cm² [6] have been reported with the technology based on a silicon platform.

Despite the advantages and advance of Si-based technology, the utility of the tunnel diodes has been limited because the functionality of tunnel diode as a two terminal NDR device is limited and the successful integration of tunnel diodes and transistors has only been possible with the III-V material systems [1,7]. In this paper, we demonstrate the first 3-terminal Si-based NDR device realized by a monolithic vertical integration of a Si-based tunnel diode

with a Si/SiGe HBT on a silicon substrate. These integrated RITD-HBT quantum functional devices have the promising characteristics of adjustable PVCR, PCD, and voltage swing corresponding to the NDR region at room temperature operation. Among these figures-of-merit, this RITD-HBT combination demonstrates that PVCR can be adjusted to be infinite or even negative and PCD can be controlled to be zero or negative. The exact control of the PVCR, and more importantly the PCD, is very important to overcome any current mismatch in bistable logic functioning circuitry. Another new feature of this integration is the capability of controlling the voltage swing in the NDR region. This third flexibility is very powerful in the radio frequency circuit applications that require the usage of the negative differential resistance of a device. A III-V-based VCO [4] using RTDs and HBTs is a prime example of what this technology offers to Si microelectronics.

STRUCTURE DESIGN AND PROCESS

The overall RITD-HBT structure, as shown in Fig. 1 (a), is designed such that the RITD structure is placed between the top emitter contact for the HBT and the emitter itself of the HBT. Here the RITD can modulate the current transport across the HBT emitter.

The RITD-HBT structures were grown by two successive epitaxial growth techniques. For the n-p-n HBT portions [8], the sub-collector doped at $2.5 \times 10^{19} \text{ cm}^{-3}$ and collector doped at $1.5 \times 10^{17} \text{ cm}^{-3}$ were grown by metal organic chemical vapor deposition (MOCVD) on 4-inch p-type substrates of which the resistivity is over 2000 $\Omega\text{-cm}$. Phosphorus was used as dopant for the sub-collector and collector growth. The base, emitter, and RITD portions were grown by molecular beam epitaxy (MBE). In the SiGe base region, which was pseudomorphically grown on the CVD-grown collector, the Ge profile was graded nominally with 30 percent of Ge at the base/collector junction and 10 percent at the emitter/base junction. The base layer, doped by Boron at $1.0 \times 10^{19} \text{ cm}^{-3}$, was sandwiched between two undoped SiGe layers of 15 nm each to minimize base dopant out-diffusion. Then, the Si emitter layer doped by phosphorus at $1.0 \times 10^{18} \text{ cm}^{-3}$ was grown atop the SiGe base layer.

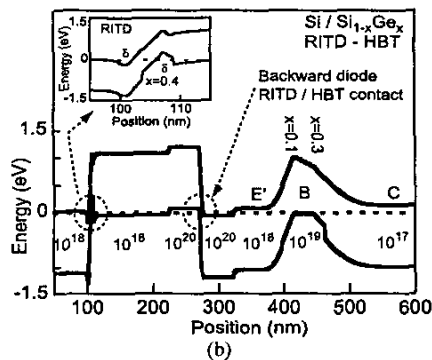
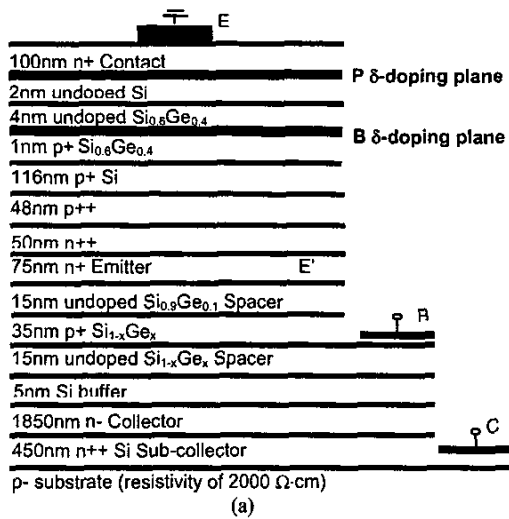


Fig 1. (a) Schematic of layer structure of the SiGe RITD with SiGe HBT (b) Calculated band diagram of RITD / HBT.

A SiGe RITD was grown atop the HBT emitter. The structure design of the Si-based RITD was based on previous work [2,6] developed by the authors. For this state-of-the-art Si-based RITD, several key points employed are: (i) δ -doped injectors to create defined quantum wells, (ii) a composite intrinsic tunneling barrier to effectively clad the δ -doped spike, (iii) low temperature MBE (LT-MBE) growth to suppress segregation and diffusion, and (iv) post-growth rapid thermal anneal (RTA) heat treatment to reduce point defects created during the LT-MBE process. Details on RITD growth are reported elsewhere [2,6]. It should be noted that only one post-growth RTA treatment at 800 °C for 1 min was performed after the completion of the RITD-HBT growth.

A special consideration has been taken to overcome the polarity mismatch in current between the RITD and HBT. A tandem of an n-on-p RITD, used here, on an n-p-n HBT is necessary to make the NDR region appear under forward active operation in the common emitter configuration. However, since both the RITD and HBT are bipolar devices, placing an n-on-p RITD directly atop the n-type HBT

emitter creates a parasitic diode between the two discrete devices that blocks current flow as it is reverse biased under forward active operation. Therefore, a highly doped p-n junction was inserted between the RITD and the emitter of the HBT acting as a short circuit reverse biased backward diode under forward active operation of the RITD-HBT tandem. The corresponding energy band diagram of the RITD-HBT structure is shown in Fig. 1 (b) generated from a semi-classical Thomas-Fermi charge calculation with the inset of RITD portion.

The fabricated RITD-HBTs employed a double mesa structure. They were fabricated using conventional photolithography and a self-aligned emitter process. Initially, the emitter metal (Cr/Au), which also acts as the anode metal for the RITD, was defined by a lift-off process. It acts as an etch mask for the emitter and RITD mesa etching. Two different wet chemical etches are required to form the emitter and RITD mesa. For a conventional SiGe HBT using a double mesa, a KOH wet etchant has been commonly used to selectively etch the Si emitter and stop etching at the SiGe base layer. However, due to the SiGe spacer layers incorporated into the RITD structure, the RITD active region was etched using the non-selective HF/HNO₃ wet etchant. Then, the etching was switched back to the selective KOH wet etchant to effectively stop at the SiGe base region. The undercut of the emitter and RITD mesa etching procedure is sufficient to provide a self-aligned base metal (Pt/Au) to the emitter mesa by shadow masking. Using a photolithographically defined photoresist etch mask to protect the self-aligned emitter-base region, the collector mesa etching was performed by the KOH wet etchant. Then the collector contact using Pt/Au was made to the n⁺ sub-collector layer by lift-off. The ohmic contacts were not annealed, but were very ohmic in nature. This may have been because a thin layer of PtSi may have been formed at the interface during electron beam evaporation due to the small heat of formation for PtSi and the potential for elevated surface temperature during deposition.

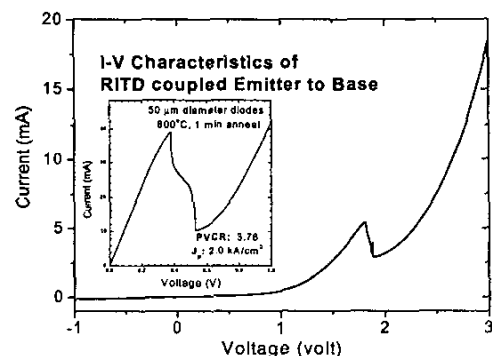


Fig 2. Measured base/emitter I-V characteristics of RITD/HBT with the collector open in which RITD and backward diode is coupled between base and emitter. Inset shows discrete RITD I-V characteristics.

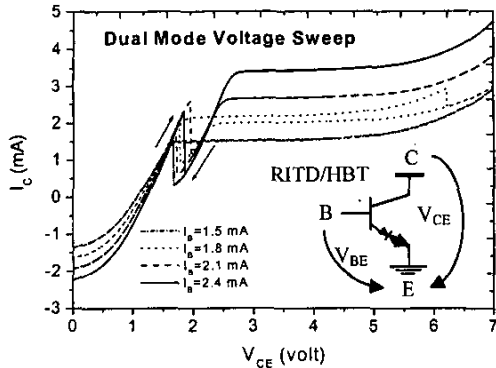


Fig 3. I-V characteristics of RITD/HBT in dual mode voltage sweep showing hysteresis in the NDR region.

RESULT AND DISCUSSION

Figure 2 shows base/emitter I-V characteristics of RITD-HBT measured at room temperature with the collector open. I-V characteristics of a discrete RITD measured separately are shown in the inset of Fig. 2. Under the common emitter configuration, for active region operation through the saturation region, the RITD is forward biased and the connecting backward tunnel diode is reverse biased, effectively shorting the RITD and emitter together.

Figure 3 shows that the collector current (I_C) versus voltage (V_{CE}) characteristics in the common emitter configuration (see inset) as a function of base current measured with dual mode voltage sweep at room temperature. The collector current characteristics showing NDR characteristics are due to the combined effects of an RITD current limiter coupled inside the HBT emitter and driven by the base current control. Since the integration results in a three-terminal NDR device, both figure-of-merits, the NDR behavior of the RITD under saturation mode for high functionality, low power, and high speed applications and the conventional active mode operation of the HBT for high speed and amplitude, can be used with respect to the bias conditions. The hysteresis observed in the NDR region of Fig. 3 when the base current rises above a

critical point results from the bistability of the RITD. Details will be discussed in the following load line analysis.

As clearly indicated in Fig. 4, the modulation of I_C versus V_{CE} using the RITD-HBT combination has shown several promising characteristics including adjustable PVCR, PCD, and the voltage swing of the NDR region. According to the definition of PVCR, the peak-to-valley current ratio can have an infinite value by tuning the valley current to zero with the control of base current. For example, the value of I_{peak} (1.7 mA) is greater by 2 orders of magnitude than that of I_{valley} (1.6×10^{-2} mA) in the 3.5 mA base current case, shown in Fig. 4. Negative values are even possible, as well as negative PCD values. To the best of author's knowledge, infinite and/or negative values have not been reported yet.

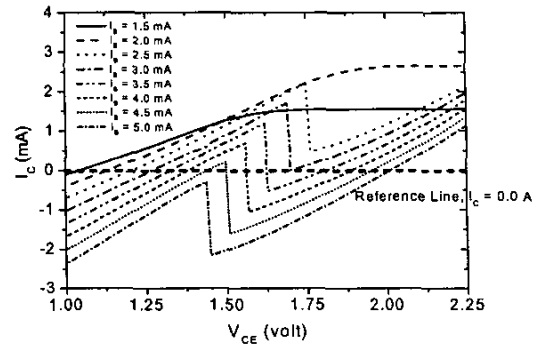


Fig 4. I-V characteristics measured demonstrate PVCR, PCD and even the voltage span can be controlled.

LOAD LINE ANALYSIS AND SWITCHING OPERATION

The integrated RITD-HBT device behavior can be explained by a load line analysis as shown in Fig. 5. Figure 5 shows the load lines of the RITD and the emitter current, I_E , for a fixed base current, I_B . The collector current is then obtained from $I_C = I_E - I_B$. For small I_B , as shown in Fig. 5 (a), the maximum forward active I_E is less than the RITD peak current. Initially, at point A the HBT is in saturation. As V_{CE} increases, the HBT enters the forward active region and the operating point becomes fixed at B. The voltage

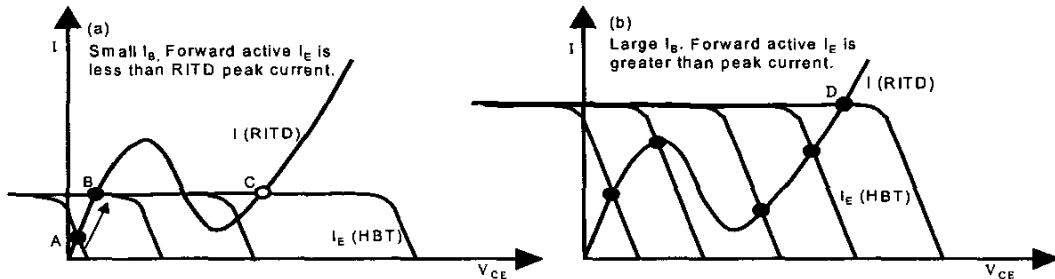


Fig. 5. RITD and HBT emitter current load lines for fixed base current, I_B . (a) Low I_B with bistable latching behavior. (b) Large I_B with infinite PVCR in I_C .

across the RITD stays fixed and further increase in V_{CE} is dropped across the HBT because I_B is fixed. Thus, no NDR is seen in the $I_C - V_{CE}$ curves for small I_B as seen in Fig. 3.

For large I_B , as shown in Fig. 5 (b), the maximum forward active I_E is greater than the RITD peak current. The HBT stays in saturation tracing out the RITD I-V, again as shown in Fig. 3. Since the HBT is saturated in the NDR region of the RITD, the base current can be adjusted to give infinite or negative PVCR in the collector current by recalling that $I_C = I_E - I_B$. This is experimentally demonstrated in Fig. 4 where I_C is observed to take on negative current values. The HBT only enters the forward active region at point D in the diffusion current turn-on of the RITD. At this point the voltage across the RITD becomes fixed and further increase in V_{CE} is dropped across the HBT.

Based on the load line analysis, switching operation using bistability due to NDR region is analyzed and demonstrated for small I_B . With the values of I_B between the peak and valley current of RITD, the integrated RITD-HBT acts as a latch because the 2 stable operating points B and C can be achieved as shown in Fig. 5 (a). The voltage V_{BE} can be used as a logic level since $V_{BE} = V_{RITD} + V'_{BE}$ where V'_{BE} is the voltage across the base emitter diode which is fixed. Starting at the low level, point A of Fig. 6 (a), switching is performed by increasing I_B until I_E is equal to the RITD peak current, point B of Fig. 6 (a). The operating point then jumps to C and the return path goes through point D and back to A. Switching operation is experimentally demonstrated in Fig. 6 (b) for a fixed V_{CE} of 3.5 V.

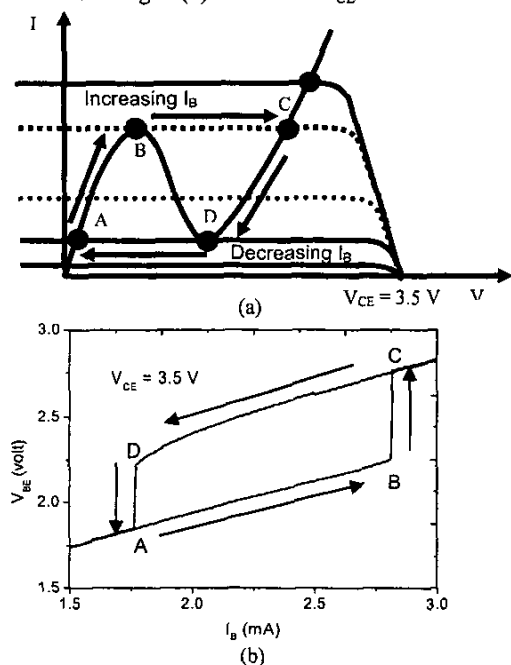


Fig. 6. Demonstration of switching operation (a) Load line analysis (b) Experimental measurement.

CONCLUSION

In conclusion, the monolithic vertical integration of Si-based RITD with SiGe HBT was demonstrated in this study. The resulting devices have the distinguishing characteristics of infinite, negative, and adjustable peak-to-valley current ratio (PVCR) with adjustable peak current density (PCD) and voltage swing corresponding to the negative differential resistance (NDR) by the control of the HBT base current. This study has also analyzed its operation as a latch and demonstrated a switching operation experimentally.

ACKNOWLEDGEMENTS

The work at Ohio State was supported by the National Science Foundation (ECS-0196208 and ECS-0196054). The work at NRL was supported by the Office of Naval Research.

REFERENCE

1. F. Capasso, S. Sen, F. Beltram, L. M. Lunardi, A. S. Vengurlekar, P. R. Smith, N. J. Shah, R. J. Malik, and A. Y. Cho, "Quantum functional devices: resonant-tunneling transistors, circuits with reduced complexity, and multiple-valued logic," *IEEE Trans. Elect. Dev.* vol. 36, No. 10 pp. 2065-2082 (1989).
2. N. Jin, S. Y. Chung, A. T. Rice, P. R. Berger, P. E. Thompson, C. Rivas, R. Lake, S. Sudirgo, J. J. Kempisty, B. Curanovic, S. L. Rommel, K. D. Hirschman, S. K. Kurinec, P. H. Chi and D. S. Simons, "Diffusion barrier cladding in Si/SiGe resonant interband tunneling diodes and their patterned growth on PMOS source/drain regions," *IEEE Trans. Elect. Dev.* vol. 50 pp. 1876-1884 (2003).
3. T. P. E. Broekaert, B. Brar, J. P. A. van der Wagt, C. Seabaugh, T. S. Moise, F. J. Morris, E. A. Beam III, and G. A. Frazier, "A monolithic 4-bit 2-Gbps resonant tunneling analog-to-digital converter," *IEEE J. Solid State Circ.*, vol. 33, pp. 1342-1349 (1998).
4. H. J. De Los Santos, K. K. Chui, D. H. Chow, H. L. Dunlap, "An efficient HBT/RTD oscillator for wireless applications," *IEEE Micro. Wireless Comp. Lett.*, vol. 11, pp. 193-195 (2001).
5. R. Duschl, and K. Eberl, "Physics and applications of Si/SiGe/Si resonant interband tunneling diodes," *Thin Solid Films*, 380, pp. 151-153 (2000).
6. N. Jin, S. Y. Chung, A. T. Rice, R. Yu, P. R. Berger, P. E. Thompson, R. Lake, "151 kA/cm² peak current densities in Si/SiGe resonant interband tunneling diodes for high power mixed-signal applications," to appear *Appl. Phys. Lett.* (October 13, 2003).
7. T. Futatsugi, Y. Yamaguchi, K. Imamura, S. Muto, N. Yokoyama and A. Shibatomi, "A resonant-tunneling bipolar transistor (RBT)-A new functional device with high current gain," *Jpn. J. Appl. Phys.*, vol. 26, No. 2 pp. L131-L133 (1987).
8. K. D. Hobart, F. J. Kub, N. A. Papanicolaou, W. Kruppa and P. E. Thompson, "Si/Si_{1-x}Ge_x heterojunction bipolar transistors with high breakdown voltage," *IEEE Elec. Dev. Lett.* vol 16, No. 5 pp 205-207 (1995).